Supplementary Material

Impact of Asian aerosols on the summer monsoon strongly modulated by regional precipitation biases

Zhen Liu[1,2], Massimo A. Bollasina[2], Laura J. Wilcox[3]

[1]Earth, Ocean and Atmospheric Sciences (EOAS) Thrust, Function Hub, The Hong Kong University of Science and Technology (Guangzhou), Guangzhou, China

[2]School of Geosciences, University of Edinburgh, UK

[3]National Centre for Atmospheric Science, Department of Meteorology, University of Reading, Reading, UK

Correspondence to Zhen Liu (henryzhenliu@hkust-gz.cn)

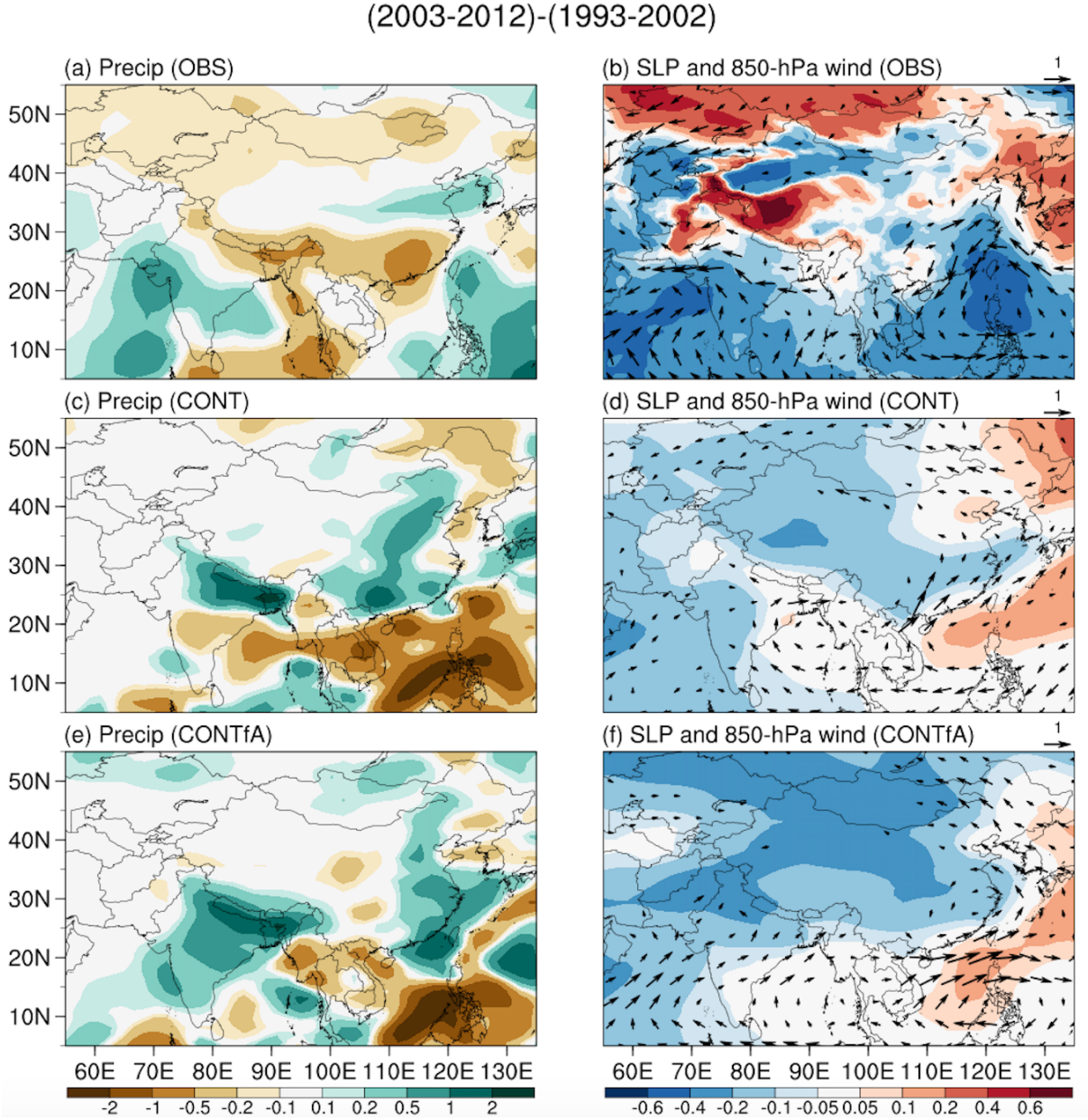

Fig. S1. The distribution of JJAS precipitation differences (mm day^{-1}) between (2003–2012) and (1993–2002) in (a) the mean of GPCP and CMAP, (b) CONT, and (c) CONTfA. (b, d, f) Same as (a, c, e) but for SLP (hPa) and 850-hPa wind (m s^{-1}) in ERA5 reanalysis and model simulations.

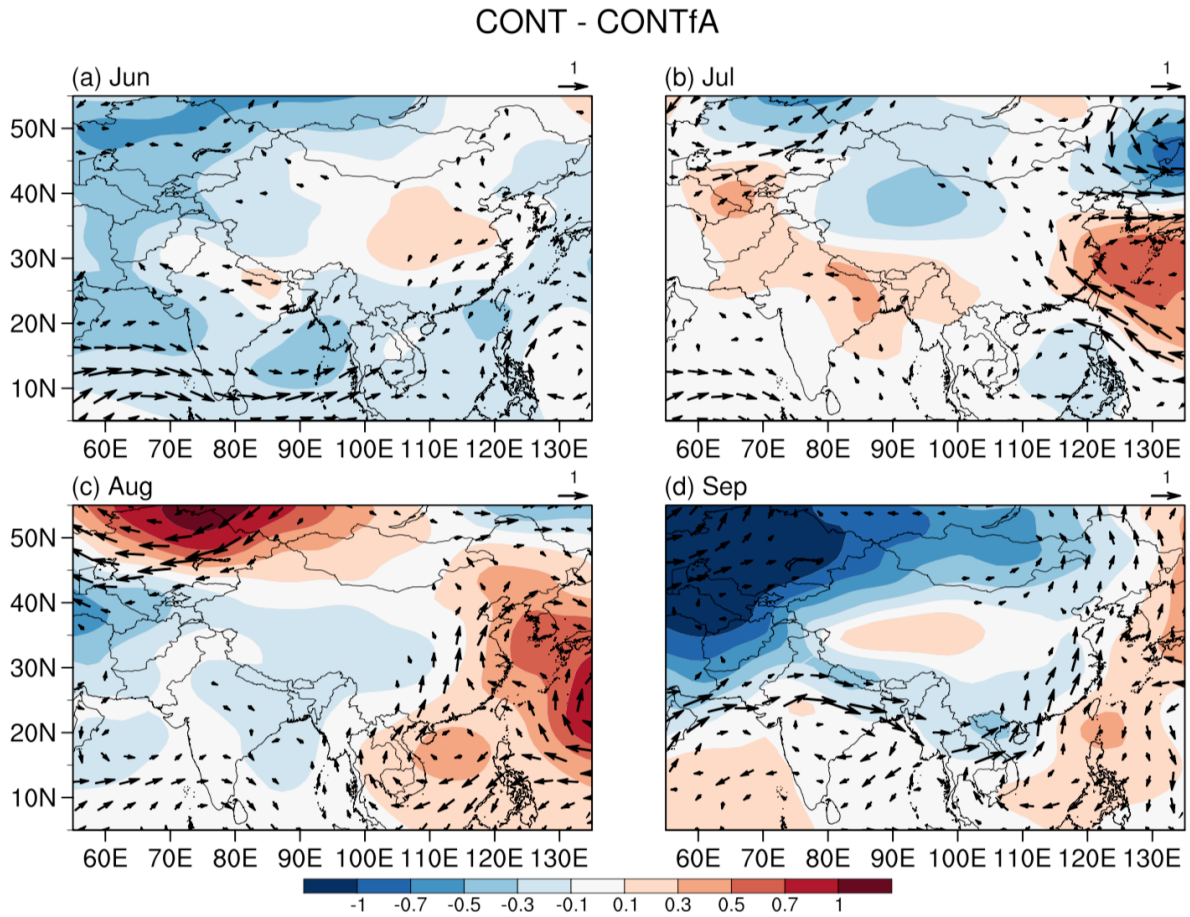

Fig. S2. Monthly differences in sea-level pressure (hPa, shades) and 850-hPa winds (m s^{-1}) between CONT and CONTfA in (a) June, (b) July, (c) August, and (d) September for the period 1993–2012.

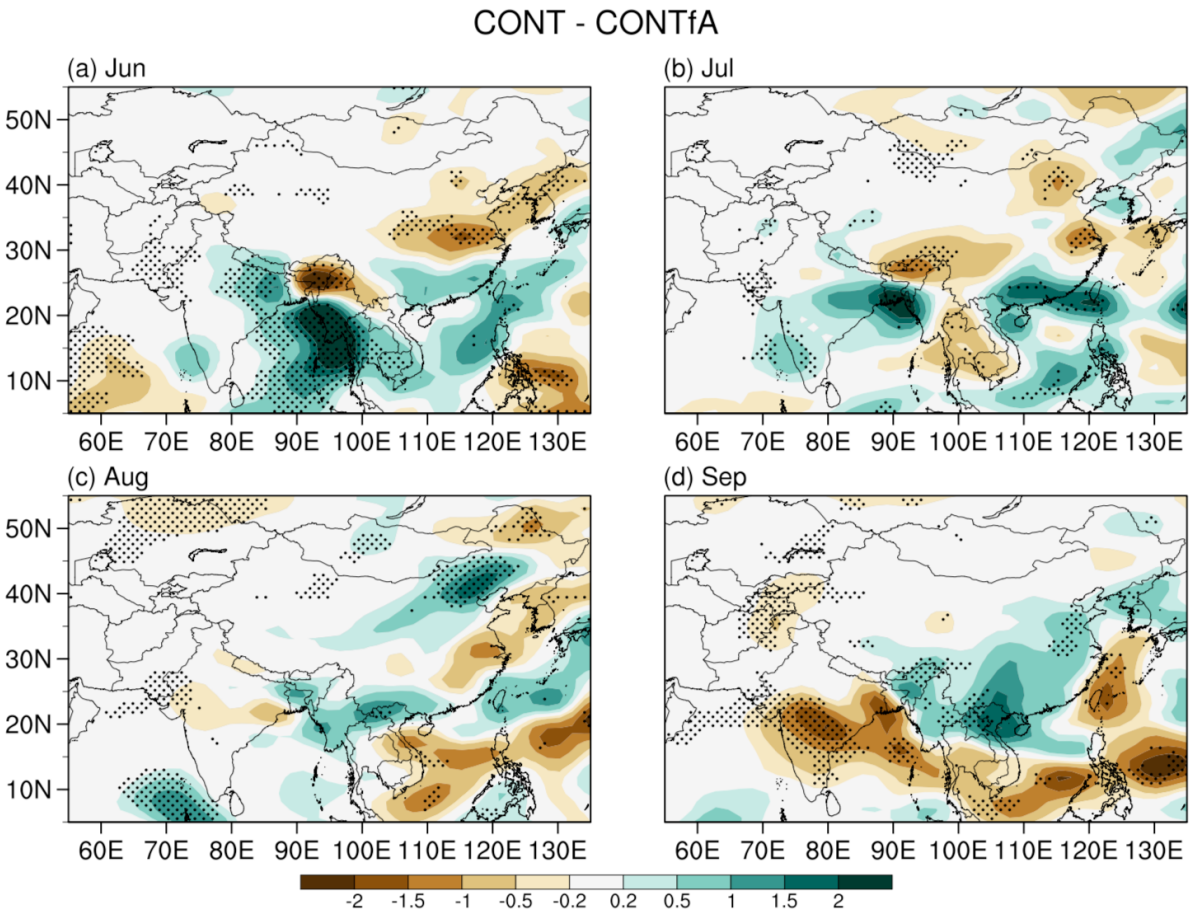

Fig. S3. Same as Fig. S2 but for precipitation (mm day^{-1}). Black dots mark grid-points for which the difference is significant at the 90% confidence level.

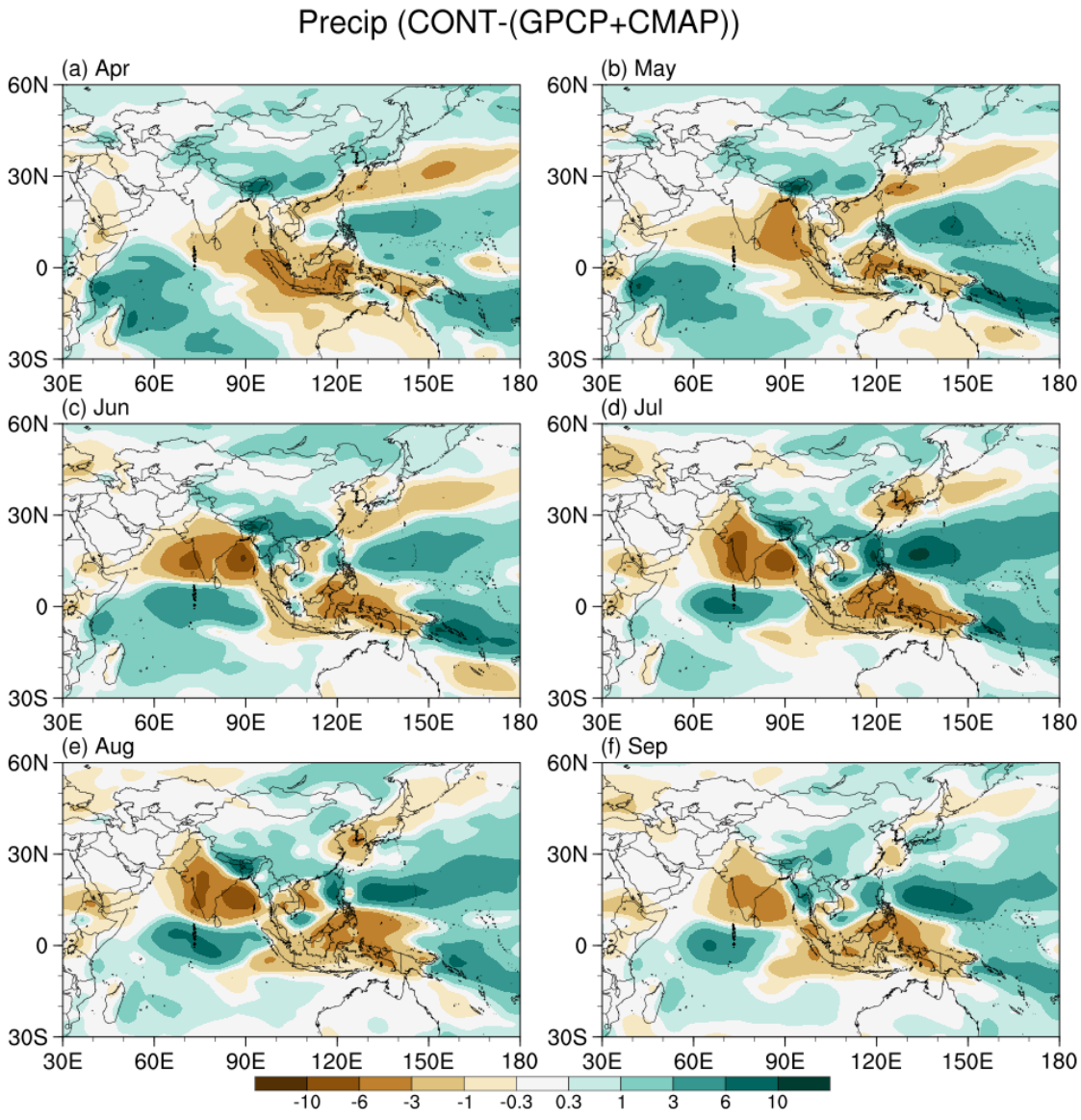

Fig. S4. Monthly precipitation bias (mm day^{-1}) in CONT with respect to the mean of GPCP and CMAP for (a) April, (b) May, (c) June, (d) July, (e) August, and (f) September.

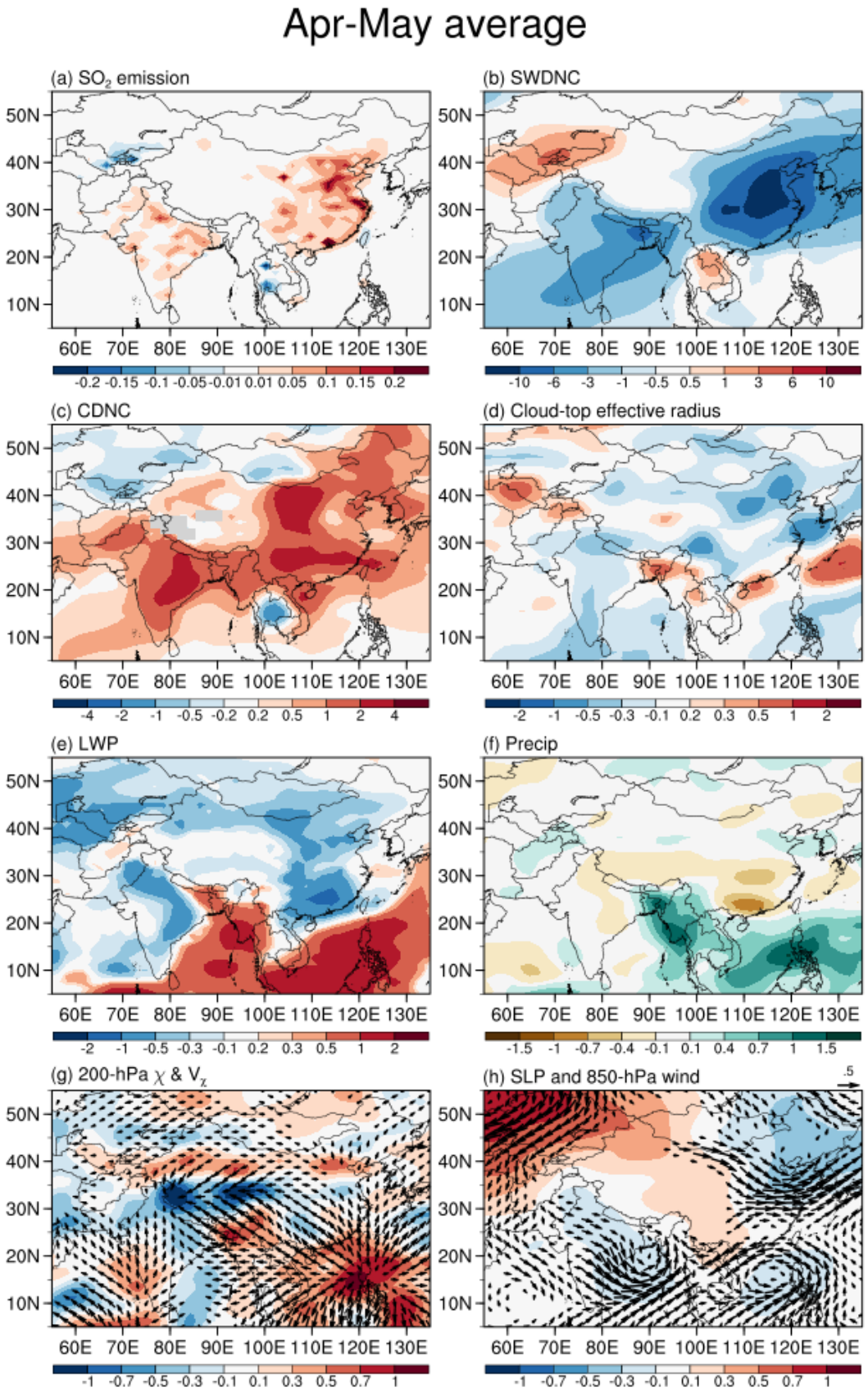

Fig. S5. April-May average differences in (a) SO_2 emissions (Tg yr^{-1}), (b) clear-sky downward shortwave radiation (W m^{-2}), (c) cloud droplet number concentration (10^{10} m^{-2}), (d) cloud-top effective radius (μm), (e) liquid water path (g m^{-2}), (f) precipitation (mm day^{-1}), 200-hPa divergence (10^6 s^{-1}, shades) and divergent wind (m s^{-1}), and (h) sea-level pressure (hPa) and 850-hPa winds (m s^{-1}) between CONT and CONTfA.

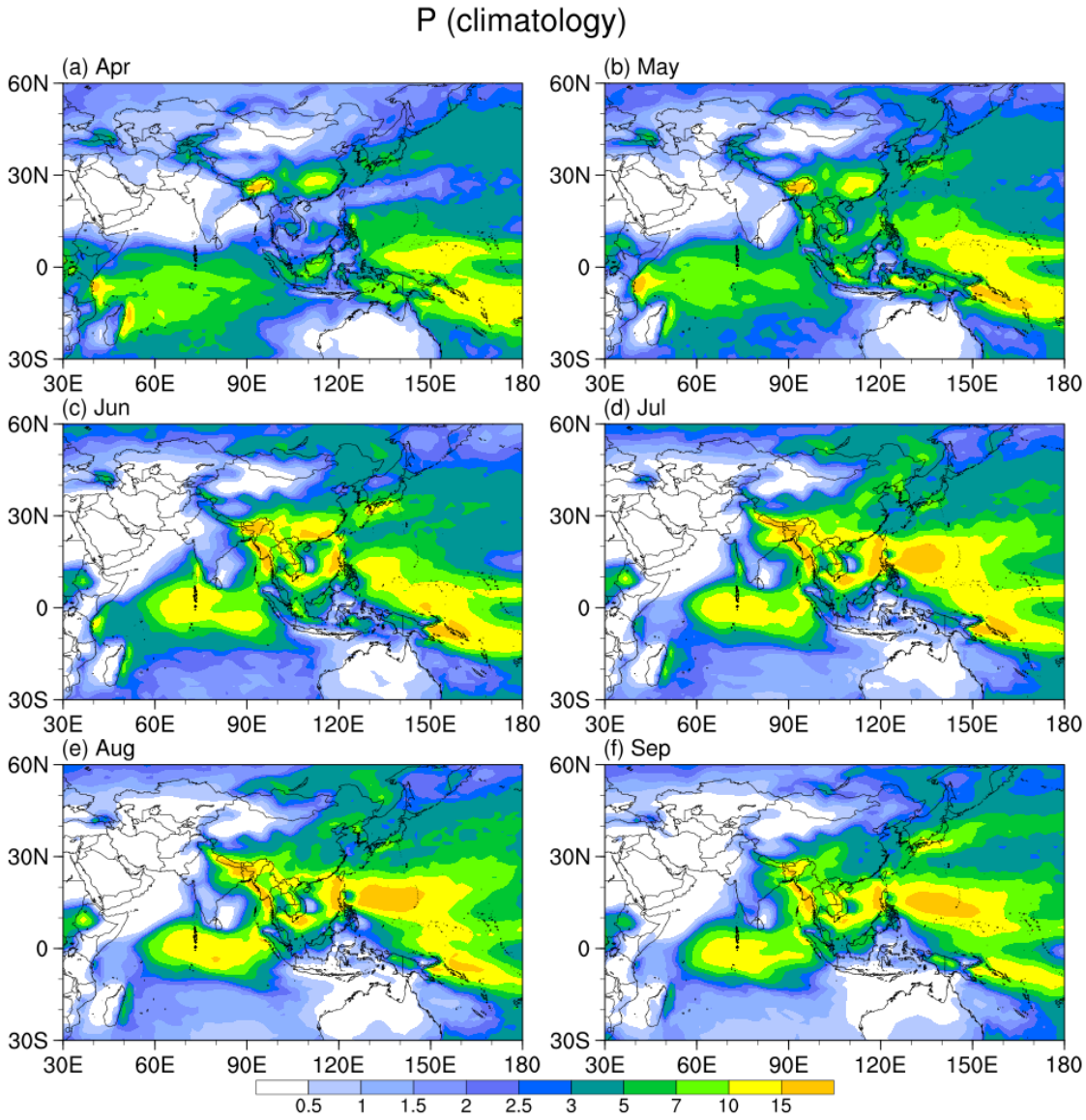

Fig. S6. CONT climatological (1981–2010 average) precipitation (mm day^{-1}) in (a) April, (b) May, (c) June, (d) July, (e) August, and (f) September.

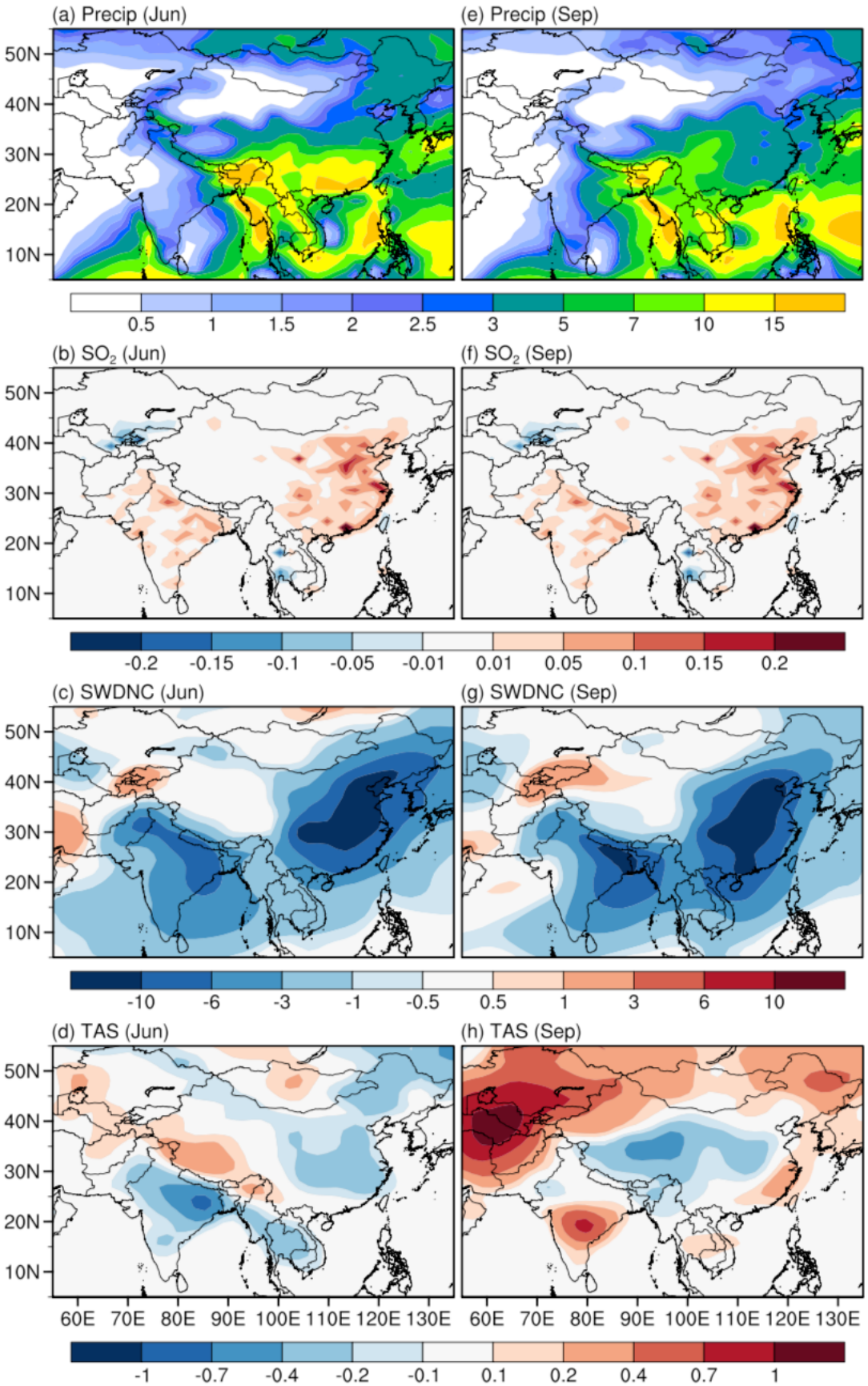

Fig. S7. (a) The June climatological precipitation (mm day^{-1}) in CONT. June differences in (b) SO_2 emissions (Tg yr^{-1}), (c) clear-sky downward shortwave radiation (W m^{-2}), and (d) near-surface temperature (K) between CONT and CONTfA. (e–h) Same as (a–d) but for September.

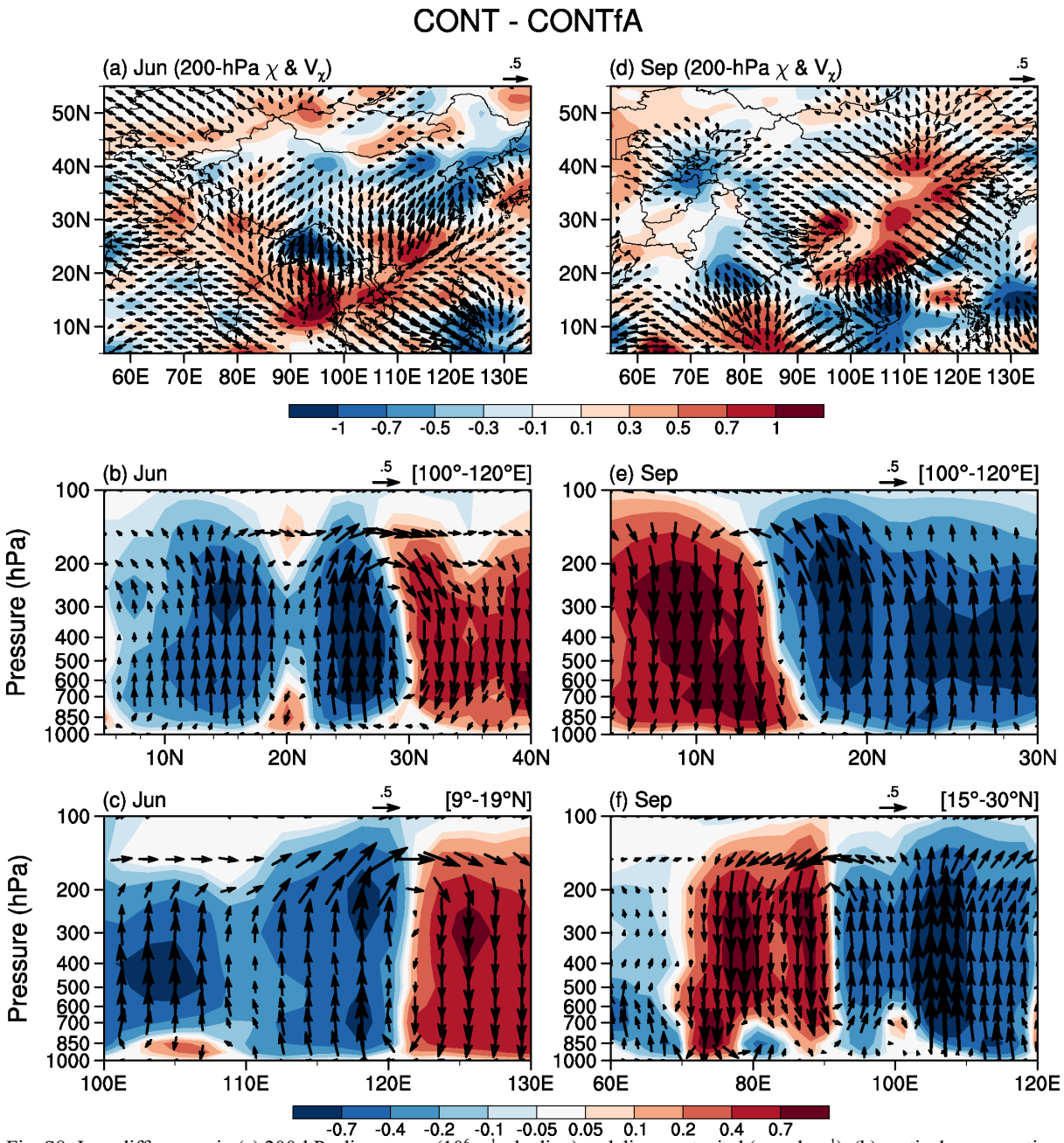

Fig. S8. June differences in (a) 200-hPa divergence (10^6 s^{-1}, shading) and divergent wind (mm day^{-1}), (b) vertical cross-section of vertical velocity (10^{-2} Pa s^{-1}) and divergent circulation averaged over 100°–120°E, and (c) over 9°–19°N. (d–f) Same as (a–c) but for September.

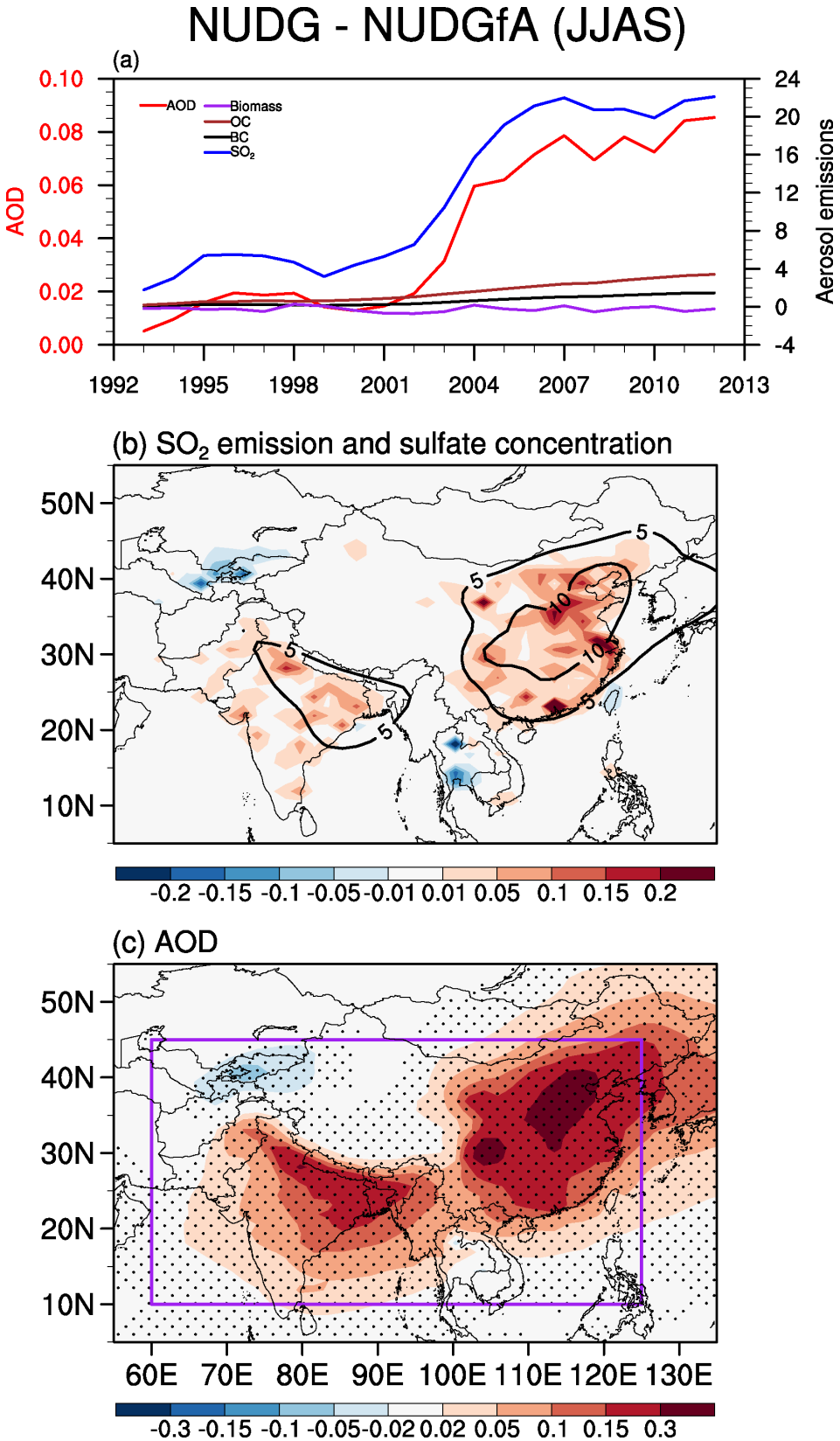

Fig. S9. Same as **Error! Reference source not found.** but for the differences between NUDG and NUDGfA.

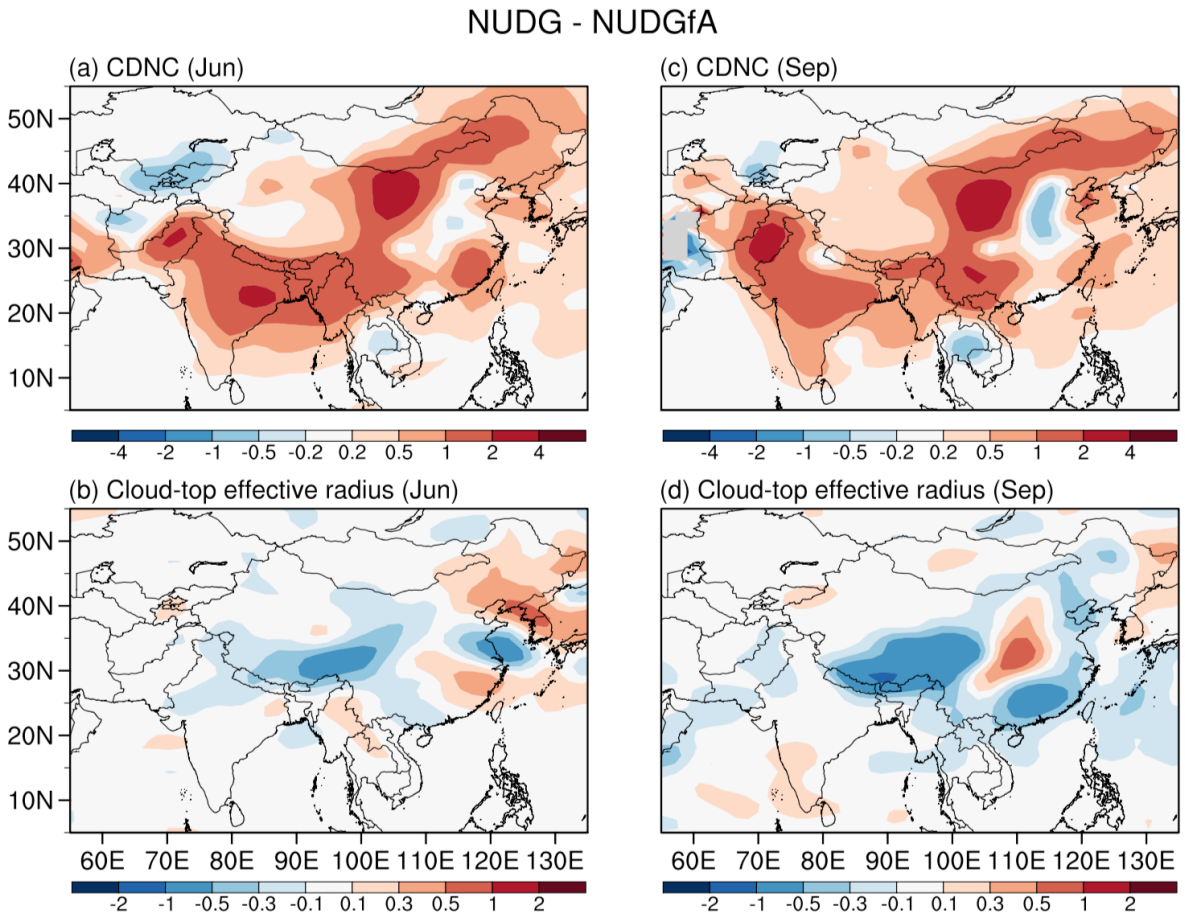

Fig. S10. June differences in (a) cloud droplet number concentration (10^{10} m^{-2}) and (b) cloud-top effective radius (μm) between NUDG and NUDGfA. (c, d) Same as (a, b) but for September.

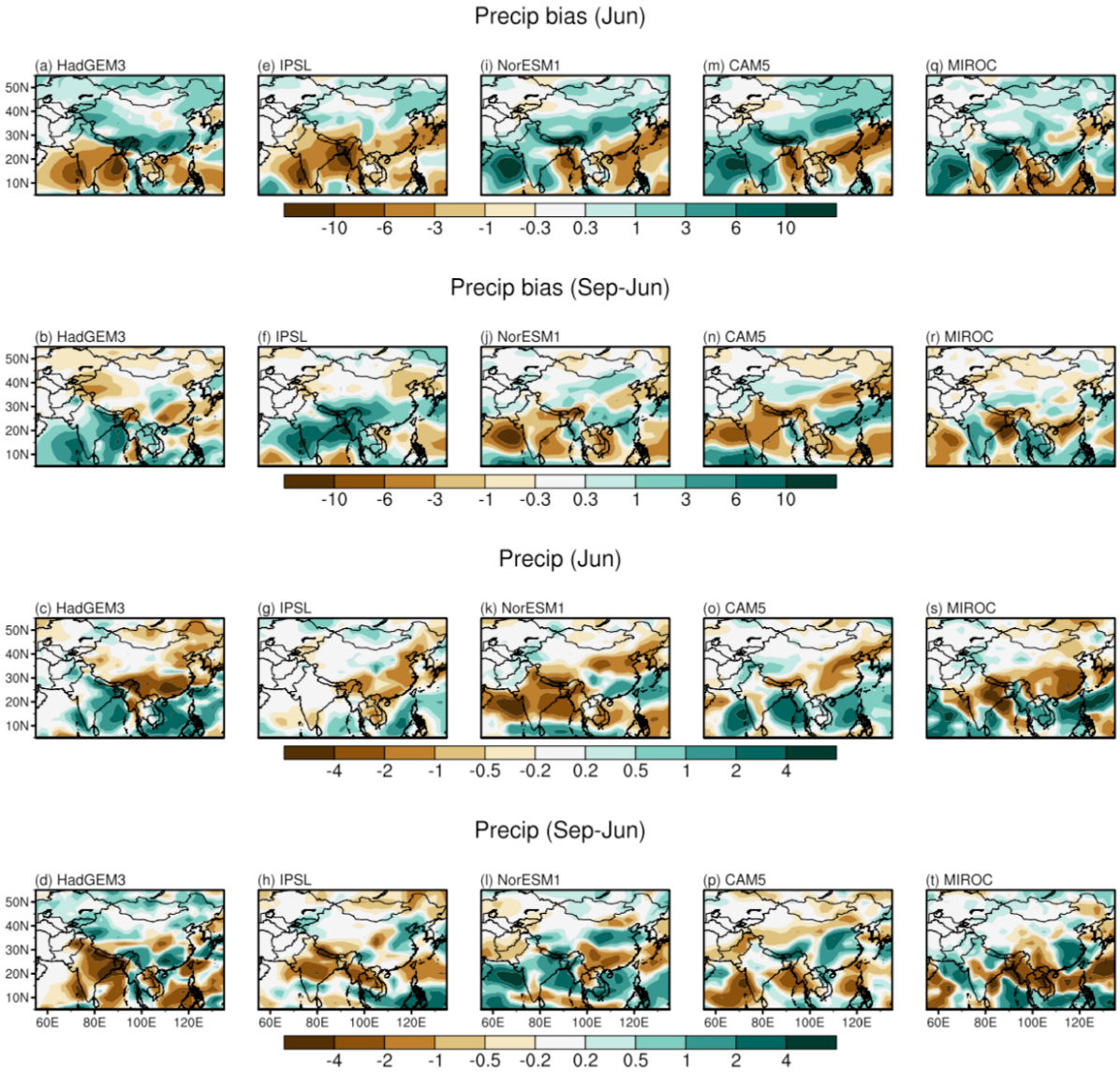

Fig. S11. From top to bottom: June precipitation bias (mm day^{-1}), September minus June difference in precipitation bias (mm day^{-1}), June precipitation response (mm day^{-1}) to increased Asian sulfate aerosols (differences in June between 10× sulfate and baseline simulations), and September minus June difference in the precipitation response to increase Asian sulfate aerosols in individual PRDMIP fixed SST models (from left to right: HadGEM3, IPSL, NorESM1, CAM5, and MIROC, respectively).

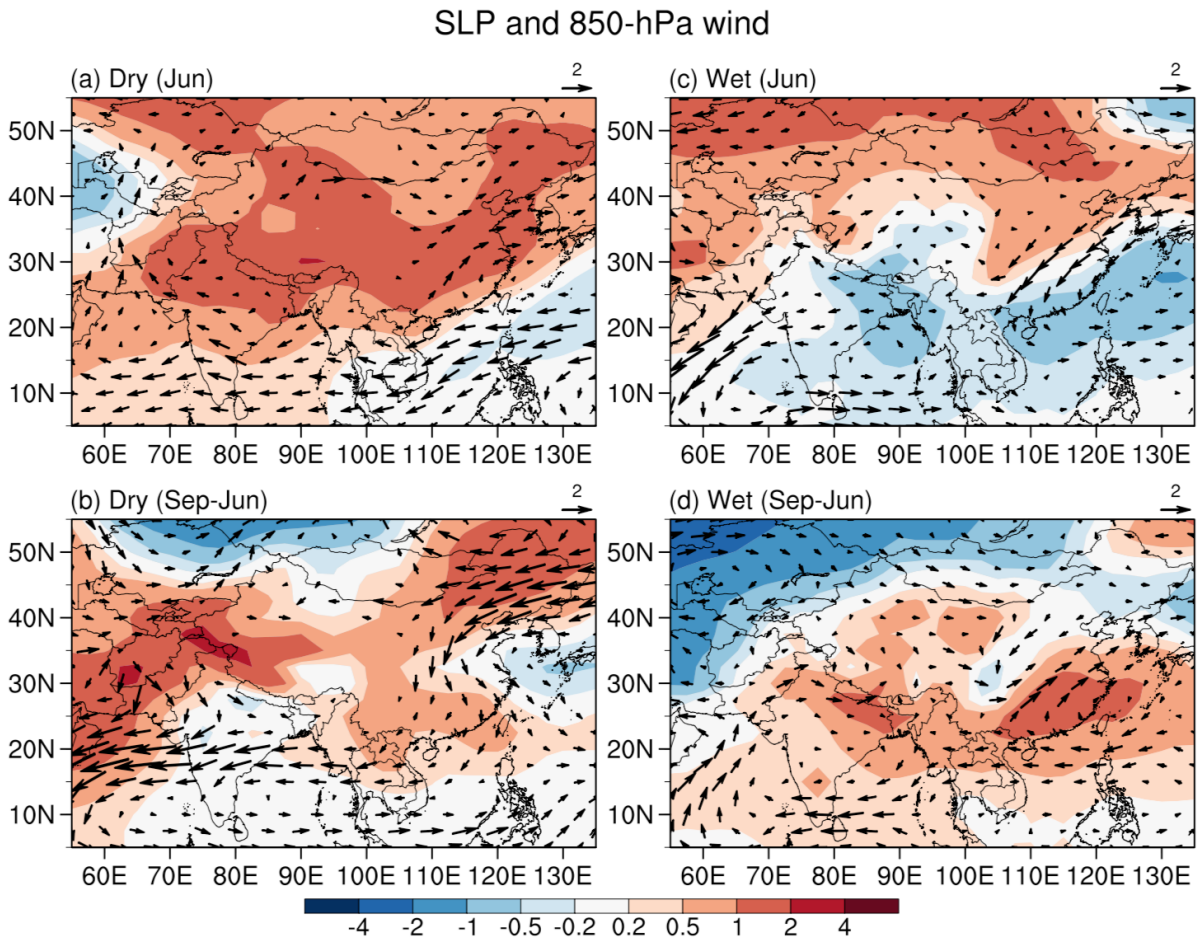

Fig. S12. Sea-level pressure (hPa, shades) and 850-hPa wind (m s^{-1}) responses to increased Asian sulfate aerosols in the (left column) DRY and (right column) WET PDRMIP model composites. (a) and (c): June, (b) and (d): September minus June differences.

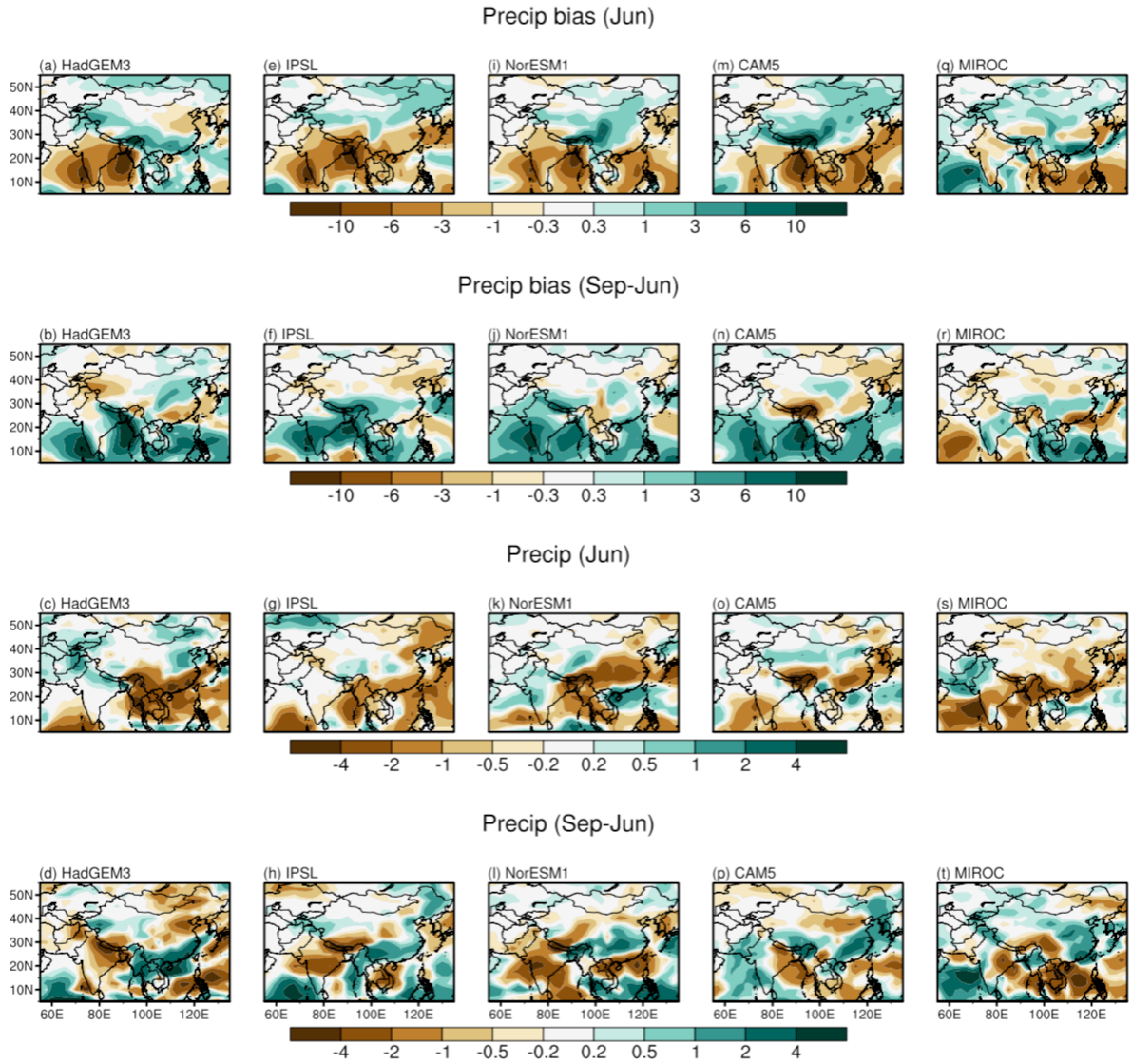

Fig. S13. As Fig. S11 but for the PDRMIP coupled models.

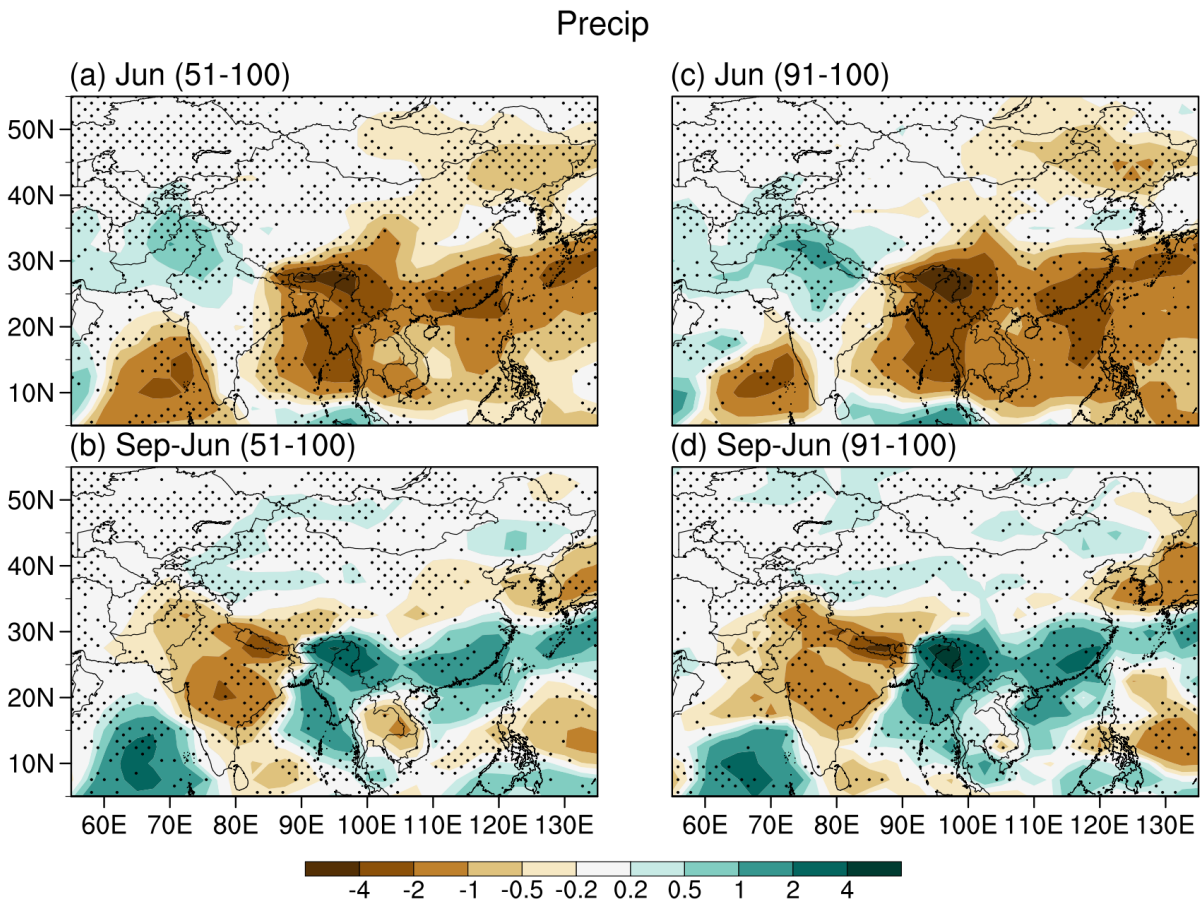

Fig. S14. PDRMIP coupled model composites in (a) June precipitation response (mm day^{-1}), and (b) the September minus June precipitation response to increased Asian sulfate aerosols (i.e., the difference between 10× sulfate and baseline simulations) averaged over the years 51–100. (c) and (d): Same as (a) and (b) but for averages over the years 91–100. Black dots mark grid-points for which at least four out of the five models agree on the sign of the precipitation differences.

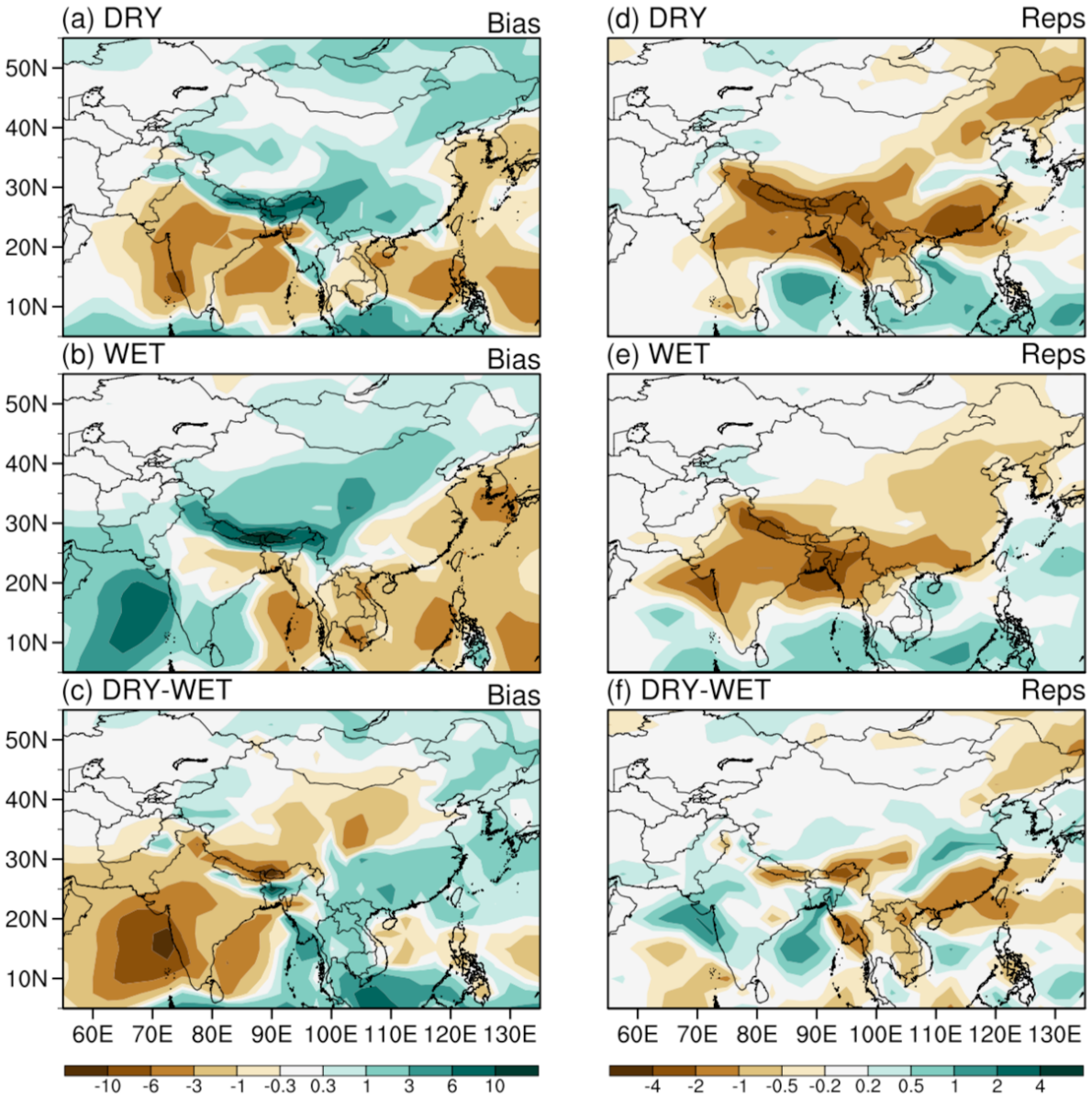

Fig. S15. Left column: Summer (JJAS) precipitation bias (mm day^{-1}) in the (a) DRY PDRMIP model composite, (b) WET model composite, and (c) difference between DRY and WET models. (d–f) Same as (a–c) but for the precipitation response to increased Asian sulfate aerosols.